AIAA AVIATION Forum
12-16 June 2023, San Diego, CA and Online
AIAA AVIATION 2023 Forum

10.2514/6.2023-4451

Shape Optimization of Hypersonic Lifting Vehicles Via Convex Relaxation

Daniel C. Berkenstock * and Juan J. Alonso†
Stanford University, Stanford, CA 94305, USA

Laurent Lessard‡
Northeastern University, Boston, MA, 02115, USA

In this paper, we extend our previous approach to the conceptual design of hypersonic aerospace vehicles, using convex optimization, to include lift as a performance indicator and constraint. Our approach employs the transformation of the lift coefficient formula to a concave function, by change of variables. This results in design problems featuring a convex objection function with a single nonconvex constraint, which we address using convex relaxation. Doing so allows us to approach a richer space of design problems which now include minimum lift constraints and treatment of lift to drag ratio within the objective function. We also apply numerical integration directly to the continuous differentials of both lift and drag, versus the panelized approach of our previous work. We demonstrate this approach on problems incorporating lift and drag, and also demonstrate a bilevel optimization problem to obtain a globally optimal maximum lift to drag coefficient vehicle.

I. Introduction

The field of Aerospace Shape Optimization (ASO) has developed significantly over the last several decades, coupling computational simulation of flow fields with optimization routines that search a design space for improved performance.

Aerodynamic performance is typically analyzed via the solution of nonlinear, nonconvex partial differential equations, which are solved using iterative techniques. These methods are often computationally expensive, curtailing their applicability in high dimensional design spaces. Even with modern methods, such as the adjoint approach to calculating gradients, these methods are often limited to the refinement of an existing design. This approach complicates the search for globally optimal performance as, in practice, a designer requires an initial guess closer to the global optimum than, potentially, many local solutions.

Convex optimization [1] is a field of mathematics that has been used to efficiently identify globally optimal solutions in many engineering disciplines. This approach has been employed in vehicle configuration design [2], however, its use in the physical design of aerodynamic vehicles has been limited [3], except for recent research exploring linearized thin airfoil theory [4] and design of low-observability hypersonic vehicles [5].

Meanwhile, the design of hypersonic vehicles has regained renewed interest in recent years, due to development of several commercial hypersonic transport vehicles and requirements for high speed weapons.

In our previous work [5], we presented an approach we call Convexity Assisted Shape Optimization (CASO). This method combines representation of shapes by explicit polynomials, defined by linear design vectors, with convex conjugates for performance assessment. Such an approach allows for the application of convex optimization to hypersonic vehicle design problems combining the minimization of drag and radar cross section. However, our previous approach did not address lift, an important performance element of vehicle design.

The remainder of this paper is organized as follows. First, we provide a brief summary of the CASO method. We then proceed to describe an approach which combines variable transformation with convex relaxation to include certain nonconvex elements within a convex programming framework. Next, we apply this approach to calculating the lift coefficient of hypersonic vehicles where Newtonian flow theory is appropriate. Finally, we demonstrate this method on several two dimensional vehicle cross section designs, including showing the Pareto front of performance tradeoff between thickness and maximum lift to drag ratio.

*PhD Candidate, Department of Aeronautics and Astronautics.
†Vance D. and Arlene C. Coffman Professor, Department of Aeronautics and Astronautics, AIAA Fellow.
‡Associate Professor, Mechanical and Industrial Engineering.

II. Convexity Assisted Shape Optimization

In Aerospace Shape Optimization (ASO), the designer attempts to optimize one, or multiple, measures characterizing performance of a physical vehicle, subject to a set of constraints on the vehicle's geometry and performance. Formally, this results in problems of the type

$$\begin{aligned} \underset{z \in D}{\text{minimize}} \quad & f_0(z) \\ \text{subject to} \quad & f_i(z) \leq 0, \quad i = 1, \ldots, m, \end{aligned} \tag{1}$$

where $z \in D$ is a vector of design variables describing the shape of the vehicle and $D \subseteq \mathbb{R}^n$ is the admissible set of variables. In a typical ASO problem, the functions, f_i, may be quite general. The objective and constraint functions are often nonlinear, nonconvex, and solved by computationally expensive, iterative methods. Additionally, there are many methods to parameterize the vehicle's shape, including discretely, by vertices and connectivity, and continuously by polynomials and/or splines that may be explicit or implicit.

The solution of problems such as shown in Equation 1 may be approached locally or globally. Global methods include algorithms such as branch-and-bound, genetic algorithms, particle swarms, and simulated annealing. These methods offer the opportunity for global optimality. However, they come at a computational cost that can be prohibitive for all but the simplest of problems. Local methods refine an initial shape towards a locally optimal solution by incorporating gradients and, often, Hessian information. Using adjoint formulations and automatic differentiation techniques, it is tractable to attempt local, gradient-based optimization even with complicated vehicle parameterizations and high-fidelity physical models. However, gradient-based optimization often proves frustrating for the designer, due to the dependency of the solution on the proximity of the initial guess. The solution may have to be repeated many times, with separate initial designs seeded across the design space, and differing parameter values fed to the optimizer. Even after repeated solutions, it may be hard to have confidence that anything approaching a global optimum has been found.

However, in a convex optimization problem, the $f_i : D \to \mathbb{R}$ must be *strictly convex*, which means that for all $0 \leq \theta \leq 1$ and $y, z \in D$ with $y \neq z$,

$$\begin{aligned} \theta y + (1-\theta) z \in D \quad & (D \text{ is a convex set}), \text{ and} \\ f(\theta y + (1-\theta) z) < \theta f(y) + (1-\theta) f(z). & \end{aligned}$$

The significant benefits of strictly convex optimization models are 1) they have a global optimum that can be found in polynomial time, 2) no special initialization is typically required, and 3) there exists a rich set of off-the-shelf solvers that require limited expertise for implementation [6, 7]. The drawback to these methods is the fact that many governing physical equations are not strictly convex.

In this work, we extend a combination of these principles we call *Convexity Assisted Shape Optimization* (CASO). There are fundamentally two observations that underly CASO. First, a rich variety of shapes may be represented by explicit polynomial splines with linear coefficients. These lend themselves easily to convex specification of geometric constraints, including thickness, area, slope, curvature, etc. The second observation is there exist approaches to modelling physical phenomena, of low to medium fidelity, that are either 1) convex, 2) nearly convex, or 3) convex over a trust region within which other information indicates the global solution should lie.

In our previous work, we described the simplest implementation of CASO. First, define a physical shape using explicit polynomial splines, with the linear coefficients as design variables. Second, identify the convex trust regions of any relevant physical phenomena. Third, develop convex surrogates for each physical phenomena by taking the maximum of a set of sampled piecewise linear functions. Fourth, combine the menu of constraints and objective functions above to develop and solve convex optimization problems resulting in globally optimal shapes.

In this paper, we extend this method to include the case of certain nonconvex elements, principally lift.

III. Aerodynamic Performance

As discussed in [8, 9], it is typical in the conceptual design of hypersonic vehicles to employ Newtonian impact theory for calculating surface pressure coefficients. Using this approach, the pressure coefficient is proportional to the squared inner product of the unit free stream velocity, $\hat{v}$, and the unit local surface normal, $\hat{n}$, over the area impinged by the flow,

$$c_p = 2(\hat{v} \cdot \hat{n})^2, \tag{2}$$

and $c_p = 0$ in regions where the flow is occluded by the body. The normal and axial force imparted to the body may then be integrated over the surface, such that

$$\begin{aligned} c_a &= -\int_{s_1}^{s_2} c_p \hat{n}_x \, \mathrm{d}s \\ c_n &= -\int_{s_1}^{s_2} c_p \hat{n}_y \, \mathrm{d}s, \end{aligned} \tag{3}$$

where, s, is the arclength along the curve. The lift and drag sectional coefficients, for angle of attack, α, are obtained as

$$\begin{aligned} c_l &= c_n \cos\alpha - c_a \sin\alpha \\ c_d &= c_n \sin\alpha + c_a \cos\alpha. \end{aligned} \tag{4}$$

So that, for $\alpha = 0$,

$$\begin{aligned} c_d &= -\int_{s_1}^{s_2} c_p \hat{n}_x \, \mathrm{d}s \\ c_l &= -\int_{s_1}^{s_2} c_p \hat{n}_y \, \mathrm{d}s. \end{aligned} \tag{5}$$

In the present paper, we will examine the case where the shape is parameterized by two explicit functions of x, representing the top and bottom surfaces, $y_{\text{upper}}(x)$ and $y_{\text{lower}}(x)$, respectively. In this case the tangent vector to the surface at any given point is $\vec{t} = \langle x, y'(x) \rangle$. The normal vector is $\vec{n} = -\hat{z} \times \vec{t} = \langle -y'(x), 1 \rangle$, which has magnitude $\|\vec{n}\| = \sqrt{1 + y'(x)^2}$. Using the derivative of arclength,

$$\mathrm{d}s = \sqrt{1 + y'(x)^2} \, \mathrm{d}x, \tag{6}$$

we find that,

$$c_d = \int_{s_1}^{s_2} -2 \frac{(-y'(x))^2}{\left(\sqrt{1 + y'(x)^2}\right)^2} \frac{(-y'(x))}{\sqrt{1 + y'(x)^2}} \sqrt{1 + y'(x)^2} \, \mathrm{d}x = 2 \int_{s_1}^{s_2} \frac{y'(x)^3}{1 + y'(x)^2} \, \mathrm{d}x. \tag{7}$$

Assuming a counter clockwise integration, (ie $\mathrm{d}x < 0$ on the lower surface and $\mathrm{d}x > 0$ on the upper surface), and a single, continuous, wetted region,

$$c_d = 2 \left[\int_0^{x_2} \frac{y'_{\text{upper}}(x)^3}{1 + y'_{\text{upper}}(x)^2} \, \mathrm{d}x - \int_{x_1}^{0} \frac{y'_{\text{lower}}(x)^3}{1 + y'_{\text{lower}}(x)^2} \, \mathrm{d}x \right]. \tag{8}$$

Similarly,

$$c_l = \int_{s_1}^{s_2} -2 \frac{(-y'(x))^2}{\left(\sqrt{1 + y'(x)^2}\right)^2} \frac{1}{\sqrt{1 + y'(x)^2}} \sqrt{1 + y'(x)^2} \, \mathrm{d}x = -2 \int_{s_1}^{s_2} \frac{y'(x)^2}{1 + y'(x)^2} \, \mathrm{d}x, \tag{9}$$

and, with the same assumptions as above.

$$c_l = 2 \left[\int_0^{x_2} \frac{-y'_{\text{upper}}(x)^2}{1 + y'_{\text{upper}}(x)^2} \, \mathrm{d}x + \int_{x_1}^{0} \frac{y'_{\text{lower}}(x)^2}{1 + y'_{\text{lower}}(x)^2} \, \mathrm{d}x \right]. \tag{10}$$

IV. Numerical Solution

Since, in practice it is difficult to obtain analytic expressions for most shapes [8], numerical integration of the lift and drag force coefficients is typically required.

One common approach is the so-called panel method, where the integral is cast as the summation of integrals over simpler, often linear, segments approximating the actual surface. Using this approach, the local normal and pressure coefficient are assumed constant over the panel.

Mathematically, for the lift on the upper surface, for instance,

$$\begin{aligned} c_{l_{\text{upper}}} &= -2\int_0^{x_2} \frac{y'_{\text{upper}}(x)^2}{1+y'_{\text{upper}}(x)^2}\,\mathrm{d}x = -2\sum_{i=0}^{N-1}\int_{x_i}^{x_i+\Delta x} \frac{y'_{\text{upper}}(x_i)^2}{1+y'_{\text{upper}}(x_i)^2}\,\mathrm{d}x \\ &= -2\sum_{i=0}^{N-1} \frac{y'_{\text{upper}}(x_i)^2}{1+y'_{\text{upper}}(x_i)^2}\int_{x_i}^{x_i+\Delta x}\mathrm{d}x = -2\Delta x\sum_{i=0}^{N-1} \frac{y'_{\text{upper}}(x_i)^2}{1+y'_{\text{upper}}(x_i)^2}. \end{aligned} \tag{11}$$

Approximating the derivative, $y'(x)$, using a forward difference,

$$y'(x_i) \approx \frac{y(x_{i+1}) - y(x_i)}{\Delta x}, \tag{12}$$

leads to the following force coefficient formulas,

$$\begin{aligned} c_l &= 2\left(\sum_{i=0}^{n/2}\frac{\Delta y_i^2|\Delta x|}{\Delta y_i^2+\Delta x^2} - \sum_{n/2+1}^{n-1}\frac{\Delta y_i^2|\Delta x|}{\Delta y_i^2+\Delta x^2}\right) \\ c_d &= 2\left(\sum_{i=0}^{n/2}\frac{\Delta y_i^3}{\Delta y_i^2+\Delta x^2} + \sum_{n/2+1}^{n-1}\frac{\Delta y_i^3}{\Delta y_i^2+\Delta x^2}\right), \end{aligned} \tag{13}$$

where $\Delta y_i = y_{i+1} - y_i$ and Δx is a constant. Note that for zero angle of attack and for a convex body, the impinged section of the surface will have $\Delta y_i \geq 0$, while $\Delta x \leq 0$ and $\Delta x \geq 0$ for the lower and upper surfaces, respectively. This approach is equivalent to rectangular integration of the underlying function and is therefore a first order method, with error, $e \propto \Delta x$.

It is also possible to achieve higher order approximations using numerical integration methods such as the trapezoidal method ($O(\Delta x^2)$ or Simpson's rule ($O(\Delta x^4)$). Using the trapezoidal rule, the integrals may be approximated as,

$$\begin{aligned} c_l =& \frac{1}{2}\left(\frac{y'_l(0)^2}{1+y'_l(0)^2} + \frac{y'_l(x_{lm})^2}{1+y'_l(x_{lm})^2}\right) + \sum_{i=1}^{N-1}\frac{y'_l(x_i)^2}{1+y'_l(x_i)^2} \\ &-\frac{1}{2}\left(\frac{y'_u(0)^2}{1+y'_u(0)^2} + \frac{y'_u(x_{um})^2}{1+y'_u(x_{um})^2}\right) - \sum_{j=1}^{M-1}\frac{y'_u(x_j)^2}{1+y'_u(x_j)^2} \\ c_d =& -\frac{1}{2}\left(\frac{y'_l(0)^3}{1+y'_l(0)^3} + \frac{y'_l(x_{lm})^2}{1+y'_l(x_{lm})^2}\right) - \sum_{i=1}^{N-1}\frac{y'_l(x_i)^3}{1+y'_l(x_i)^2} \\ &+\frac{1}{2}\left(\frac{y'_u(0)^3}{1+y'_u(0)^2} + \frac{y'_u(x_{um})^3}{1+y'_u(x_{um})^2}\right) + \sum_{j=1}^{M-1}\frac{y'_u(x_j)^3}{1+y'_u(x_j)^2}. \end{aligned} \tag{14}$$

V. Design Problem Characterization

In general, the force equations presented in the previous section lead to difficult, NP hard problems in attempting their use in design of physical shapes. These formula are rational, non-convex, and nonlinear. However, there are several avenues available to improve their tractability.

A. Shape Definition

A wide variety of shape descriptors may be modeled as the inner product of a linear design variable vector with a set of basis functions, including polynomials and polynomial splines. For example, the cubic polynomial,

$$y(x) = ax^3 + bx^2 + cx + d \tag{15}$$

is a linear function of the variables, $\vec{z} = \langle a, b, c, d\rangle$, for given x, as are it's derivatives. Since the composition of an a convex function with a linear function is convex, any convex $f(y'(x))$, will be convex when the shape is modeled as such.

B. Convex Approximation

Each of the numerical integration formulations may be modeled as,

$$F = \int_{x_0}^{x_1} f(y'(x))\,\mathrm{d}x = \sum_{i=0}^{N} w_i f(y'(x)), \tag{16}$$

with constant weight, w_i, applied to each panel depending on Δx and the numerical integration scheme. Since summation preserves convexity and the composition of a convex function with a linear function is convex, the force components will be convex or concave functions if $f(y'(x))$ is, or is approximated by, a convex or concave function. Examining the second derivative of the infinitesimal drag function, $f(y') = y'^3/(1+y'^2)$,

$$\frac{\mathrm{d}^2 f}{\mathrm{d}y'^2} = -\frac{2y'(y'^2-3)}{(1+y'^2)^3}, \tag{17}$$

we see that it is convex over the domain, $0 \le y' \le \sqrt{3}$. However, even beyond $y = \sqrt{3}$, the absolute value of the second derivative remains quite small, with a maximum value at $y'(1+\sqrt{2}) = \frac{1}{\sqrt{2}} - \frac{3}{4}$. This makes the hypersonic drag coefficient an excellent candidate for approximation by a convex surrogate function, especially in the highly likely case that, for hypersonic vehicles, the local surface inclination angle remains less than $\pi/3$. We previously showed how to represent this surrogate function as the maximum over a set of piecewise linear functions. In order to maintain simplicity in describing the current approach, we also point out that the Taylor series expansion of this function about $y'(x) = 0$ is

$$f(y') = y'^3 - y'^5 + y'^7 + O(y'^9). \tag{18}$$

Similarly, we note that the second derivative of the infinitesimal lift function, $f(y') = y'^2/(1+y'^2)$, is

$$\frac{\mathrm{d}^2 f}{\mathrm{d}y'^2} = \frac{2(1-3y^2)}{(1+y^2)^3}. \tag{19}$$

In this case we note that the function is convex over the domain, $0 \le y' \le 1/\sqrt{3}$. In addition, the first several terms of the Taylor series are,

$$f(y') = y'^2 - y'^4 + y'^6 - y'^8 + O(y'^9). \tag{20}$$

C. Variable Transformation

In addition to introducing convex approximations and simplifying shape descriptors, certain functions admit a variable transformation that converts a nonconvex function to a convex one. For the case of the hypersonic infinitesimal lift coefficient, introducing the change of variable, $r = y'^2$, leads to the function,

$$f(r) = \frac{r}{1+r} = 1 - \frac{1}{1+r}. \tag{21}$$

This function is strictly concave over the domain, $r \ge 0$, however, the constraint that $r = y'^2$ is nonconvex. In this case, we have exchanged a nonconvex performance indicator for a concave performance indicator with a nonconvex constraint.

VI. Application to Hypersonic Design

In order to apply the concepts of the previous sections to physical shape design problems, in this section we derive detailed formulations of the cubic polynomial approach to shape representation, including important boundary conditions. We then turn to truncating the Taylor series of the previous section to identify convex drag and concave lift approximations, suitable to constraints on the minimum lift to drag ratio of the body.

A. Vehicle Cross Section Definition

For current purposes we will assume modeling the upper and lower surfaces, $y_{\mathrm{upper}}(x)$ and $y_{\mathrm{lower}}(x)$ as cubic polynomials over the domain $0 \le x \le 1$. In order to simplify the analysis we will assume that both $y_{\mathrm{upper}}(x) \ge 0$ and $y_{\mathrm{lower}}(x) \ge 0$ over the domain, with the actual physical shape equal to the negative reflection of $y_{\mathrm{lower}}(x)$ about the x axis. Furthermore, we will assume that the shape (as is common in hypersonic vehicles) does not need to be closed at

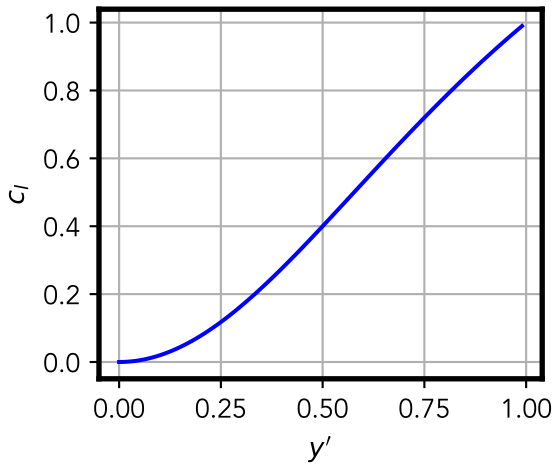

a) Original lift coefficient formulation

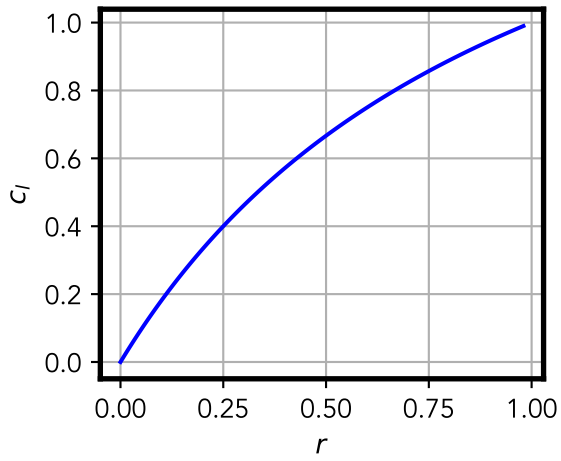

b) Transformed, concave lift coefficient formulation

Fig. 1 Original and transformed infinitesimal lift coefficient.

the trailing edge, but may have gap of $y_{\text{upper}}(1) - y_{\text{lower}}(1) \geq \tau$, where $\tau \geq 0$. Also, we will constrain the slope of the upper and lower surfaces as $y'_{\text{upper}}(1) = 0$ and $y'_{\text{lower}}(1) = 0$. This results in the following,

$$\begin{aligned} y_{\text{upper}}(x) &= ax^3 + bx^2 + cx + d \\ y_{\text{lower}}(x) &= ex^3 + fx^2 + gx + h. \end{aligned} \tag{22}$$

Since the two curves must meet at the leading edge, $x = 0$, it follows naturally that $d = h = 0$. In addition, the conditions that $y'_{\text{upper}}(1) = y'_{\text{lower}}(1) = 0$ lead to,

$$\begin{aligned} 3a + 2b + c &= 0 \\ 3e + 2f + g &= 0, \end{aligned} \tag{23}$$

resulting in an updated definition for the two curves as,

$$\begin{aligned} y_{\text{upper}}(x) &= ax^3 + bx^2 - (3a + 2b)x \\ y_{\text{lower}}(x) &= ex^3 + fx^2 - (3e + 2f)x. \end{aligned} \tag{24}$$

Similarly, the gap condition leads to,

$$-2a - b - 2e - f \geq \tau, \tag{25}$$

resulting in a shape with 3 degrees of freedom. Furthermore, we will constrain both shapes to be convex, in other words for their second derivative to be less than or equal to zero at $x = 1$,

$$\begin{aligned} 3a + b &\leq 0 \\ 3e + f &\leq 0. \end{aligned} \tag{26}$$

This dramatically simplifies the integration limits by ensuring that the integration of lift and drag forces over both the upper and lower surfaces will run from $x = 0$ to $x = 1$.

B. Convex Performance Approximation

In the present analysis, we will model lift and drag as truncated Taylor series. Our approach is easily extensible to convex and concave surrogates using maxima (or minima) over sets of piecewise linear functions.

We model the infinitesimal drag contribution as,

$$\frac{\mathrm{d}c_d}{\mathrm{d}x} = 2\frac{y'(x)^3}{1+y'(x)^2} \approx 2y'(x)^3. \tag{27}$$

Similarly, we model the lift on the upper surface, which will generally be small as it provides a negative contribution, as

$$\frac{\mathrm{d}c_{l_{\text{upper}}}}{\mathrm{d}x} = -2\frac{y'(x)^2}{1+y'(x)^2} \approx -2y'(x)^2, \tag{28}$$

and the lift on the lower surface, where it provides a positive and, likely larger, contribution as,

$$\frac{\mathrm{d}c_{l_{\text{lower}}}}{\mathrm{d}x} = -2\frac{y'(x)^2}{1+y'(x)^2} \approx 2\left(y'(x)^2 - y'(x)^4\right). \tag{29}$$

Taking these formulas, and noting that $y'(x) \geq 0$ for our definitions of both the upper and lower surface, we have,

$$\begin{aligned} c_d &= \int_0^1 2\left(y'_{\text{lower}}(x)^3 + y'_{\text{upper}}(x)^3\right)\mathrm{d}x \\ &= -2\left[\frac{432a^3}{35} + \frac{99a^2b}{5} + \frac{54ab^2}{5} + 2b^3 + \frac{432e^3}{35} + \frac{99e^2f}{5} + \frac{54ef^2}{5} + 2f^3\right] \end{aligned} \tag{30}$$

Although this is a convex function for $a \leq 0, b \leq 0$, it may be represented in a simpler (and disciplined convex [10]) format as,

$$c_d = -2\left(\sqrt[3]{\frac{432}{35}}a + \sqrt[3]{2}b\right)^3 - 2\left(\sqrt[3]{\frac{432}{35}}e + \sqrt[3]{2}f\right)^3 + \epsilon(a,b,e,f), \tag{31}$$

where the error term, $|\epsilon|$ is,

$$|\epsilon| = 2\left(\frac{99}{5} - \frac{216}{\sqrt[3]{1225}}\right)a^2b + 2\left(\frac{54}{5} - \frac{36}{\sqrt[3]{35}}\right)ab^2 \approx 0.8a^2b + 0.4ab^2. \tag{32}$$

Similarly, combining the upper and lower surface lift contributions, we see that,

$$c_l = \int_0^1 2\left(y'_{\text{lower}}(x)^2 - y'_{\text{lower}}(x)^4 - y'_{\text{upper}}(x)^2\right)\mathrm{d}x. \tag{33}$$

Noting that the second and third terms are concave, we will separate this and introduce a change of variables, such that,

$$c_l = 2\left[\int_0^1 y'_{\text{lower}}(x)^2\,\mathrm{d}x - \int_0^1 y'_{\text{lower}}(x)^4\,\mathrm{d}x - \int_0^1 y'_{\text{upper}}(x)^2\,\mathrm{d}x\right]. \tag{34}$$

For the first term, we will introduce the change of variables,

$$r = 2\int_0^1 y'_{\text{lower}}(x)^2\,\mathrm{d}x, \tag{35}$$

Examining the second term,

$$-2\int_0^1 y'_{\text{lower}}(x)^4\,\mathrm{d}x = -2\left[\frac{1152}{35}e^4 + \frac{2511}{35}e^3f + \frac{2088}{35}e^2f^2 + \frac{112}{5}ef^3 + \frac{16}{5}f^4\right] \tag{36}$$

$$= -2\left(\sqrt[4]{\frac{1152}{35}}e + \sqrt[4]{\frac{16}{5}}f\right)^4 + \epsilon(e,f), \tag{37}$$

where,

$$|\epsilon| \approx 3.54e^3f + 3.84e^2f^2 + 1.05ef^3 \tag{38}$$

With respect to the third term,

$$-2\int_0^1 y'_{\text{upper}}(x)^2\,\mathrm{d}x = -2\left(\frac{24}{5}e^2 + 5ef + \frac{4}{3}f^2\right), \tag{39}$$

we note that this may be represented as the quadratic form,

$$-2\left(\frac{24}{5}e^2 + 5ef + \frac{4}{3}f^2\right) = -2\begin{bmatrix} e & f \end{bmatrix}\begin{bmatrix} \frac{24}{5} & \frac{5}{2} \\ \frac{5}{2} & \frac{4}{3} \end{bmatrix}\begin{bmatrix} e \\ f \end{bmatrix} = -2z^T C z. \tag{40}$$

As the eigenvalues of the matrix, $\lambda(C) = \frac{1}{30}\left(92 \pm \sqrt{8329}\right) \geq 0$ it follows that the negation of this quadratic form is negative definite and, therefore, concave.

Combining terms, we reach a final formulation for lift as,

$$c_l = r - 2\left(\sqrt[4]{\frac{1152}{35}}e + \sqrt[4]{\frac{16}{5}}f\right)^4 - 2\begin{bmatrix} a & b \end{bmatrix}\begin{bmatrix} \frac{24}{5} & \frac{5}{2} \\ \frac{5}{2} & \frac{4}{3} \end{bmatrix}\begin{bmatrix} a \\ b \end{bmatrix}. \tag{41}$$

And, now, have constructed convex approximations for both lift and drag suitable for use in standard, open-source, convex optimization solvers.

VII. Design Case Studies

In the current section, we demonstrate three applications of the design approach outlined above. First, we demonstrate the minimization of drag, a strictly convex problem. Second, we show the ability to design a shape with a given lift to drag ratio, a nonconvex problem tightly relaxed to a convex problem. Finally, we describe a bi-level approach to obtaining a shape of maximum lift to drag ratio using an outer golden section search method, with an inner convex optimization problem.

A. Drag Minimization

Our first case study is a strictly convex optimization problem, minimizing the approximate drag of a two dimensional, hypersonic vehicle cross section subject to minimum area and thickness constraints.

$$\begin{aligned} \underset{\langle a,b,e,f\rangle}{\text{minimize}} \quad & -2\left(\sqrt[3]{\frac{432}{35}}a + \sqrt[3]{2}b\right)^3 - 2\left(\sqrt[3]{\frac{432}{35}}e + \sqrt[3]{2}f\right)^3 \\ \text{subject to} \quad & 3a + b \leq 0 \\ & 3e + f \leq 0 \\ & -2a - b - 2e - f \geq \tau \\ & -\frac{5}{4}a - \frac{2}{3}b - \frac{5}{4}e - \frac{2}{3}f \geq A_{\min}. \end{aligned} \tag{42}$$

For the case $\tau = A_{\min} = 0.125$, the minimum estimated drag is 0.0062 and the actual calculated drag via numerical integration is 0.0061. In this case, $a = e = -0.05$ and $b = f = -6.02\text{e}{-7}$, and the active constraint is the area. The calculated thickness at $x = 1$ is 0.125.

B. Lift to Drag Ratio Constraint

The second design case study demonstrates the optimization of a vehicle cross section given a minimum lift to drag ratio. Here, the lift is modeled as a concave function, with an added relaxation of a nonconvex, quadratic equality constraint and the objective function minimizes the value of the relaxation variable.

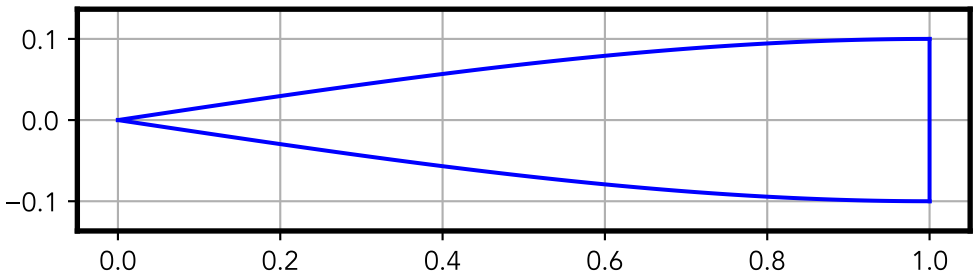

Fig. 2 Minimum drag shape for $\tau = A_{\min} = 0.125$.

$$
\begin{aligned}
\underset{\langle a,b,e,f\rangle}{\text{minimize}} \quad & r^2 \\
\text{subject to} \quad & -\left[\left(\sqrt[3]{\frac{432}{35}}a + \sqrt[3]{2}b\right)^3 + \left(\sqrt[3]{\frac{432}{35}}e + \sqrt[3]{2}f\right)^3\right](\mathrm{L/D}_{\min}) \\
& -\left[r - \left(\sqrt[4]{\frac{1152}{35}}e + \sqrt[4]{\frac{16}{5}}f\right)^4 - \begin{bmatrix} a & b \end{bmatrix}\begin{bmatrix} \frac{24}{5} & \frac{5}{2} \\ \frac{5}{2} & \frac{4}{3} \end{bmatrix}\begin{bmatrix} a \\ b \end{bmatrix}\right] \leq 0 \\
& \begin{bmatrix} e & f \end{bmatrix}\begin{bmatrix} \frac{24}{5} & \frac{5}{2} \\ \frac{5}{2} & \frac{4}{3} \end{bmatrix}\begin{bmatrix} e \\ f \end{bmatrix} \leq r \\
& 3a + b \leq 0 \\
& 3e + f \leq 0 \\
& -2a - b - 2e - f \geq \tau.
\end{aligned} \tag{43}
$$

Here, the prescribed parameters, $\mathrm{L/D}_{\min} = 1.0$ and $\tau = 0.125$, result in $a = -3.00\text{e}{-3}$, $b = -9.38\text{e}{-6}$, $e = -3.26\text{e}{-3}$, and $f = -1.04\text{e}{-5}$, with the lift and drag values shown in Table 1. The relaxation is tight in this instance, with a relaxation error of $\epsilon = 5.20\text{e}{-8}$. This is important as it gives an important confirmation whether or not we have actually solved for the global optimum. In the case, where the relaxation is not tight, the solution will be physically meaningless as r will not accurately reflect the portion of lift contributed on the lower surface by the y' term.

	Convex Approximation	Numerical Integration	Error
c_l	1.515e−3	1.583e−2	4.3%
c_d	1.515e−3	1.520e−3	0.3%
L/D	1.00	1.04	4.0%

Table 1 Convex approximation vs numerical integration values of force coefficients.

C. Lift to Drag Ratio Maximization

As a final design case study, we employ a bi-level approach to identify the globally optimal cross section, given a minimum trailing edge thickness.

First, we construct a nonconvex, but unimodal, objective function that accounts for both the calculated lift to drag ratio as well as any relaxation error. We do so by dividing the calculated lift to drag ratio by the greater value between a

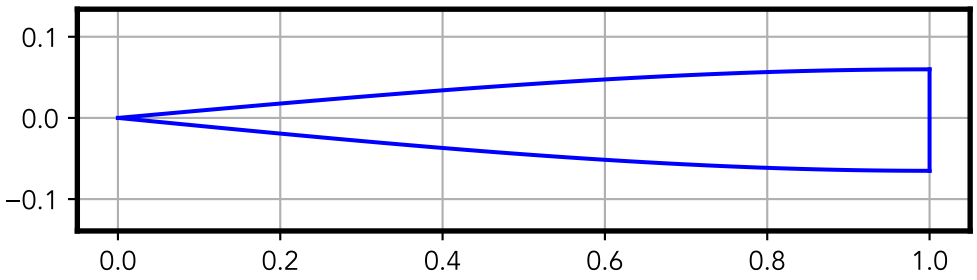

Fig. 3 Minimum relaxation error shape for $\mathrm{L/D_{min}} = 2.5$ and $\tau = 0.2$.

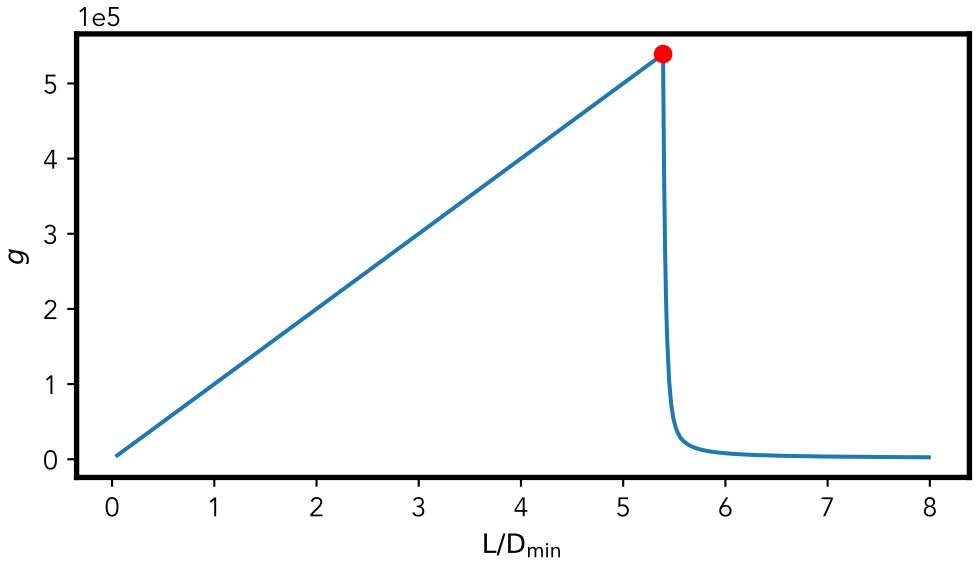

Fig. 4 Objective function g for maximizing ratio of $\mathrm{L/D}$ to normalized error, maximum indicated by red dot.

specified ϵ term or the present relaxation error,

$$r_{\text{error}} = \left| r - \begin{bmatrix} e & f \end{bmatrix} \begin{bmatrix} \frac{24}{5} & \frac{5}{2} \\ \frac{5}{2} & \frac{4}{3} \end{bmatrix} \begin{bmatrix} e \\ f \end{bmatrix} \right|. \tag{44}$$

Based on numerical experiments, we employ the value $\epsilon = 1\text{e}{-5}$. This objective function rises linearly as long as $r_{\text{error}} \leq \epsilon$. Once $r_{\text{error}} \geq \epsilon$, the objective function value drops precipitously. Hence, we seek to maximize the objective function,

$$\underset{\langle \mathrm{LD_{min}} \rangle}{\text{maximize}} \qquad g = \frac{c_l/c_d}{\max \langle \epsilon, r_{\text{error}} \rangle}, \tag{45}$$

which we accomplish via a golden-section search over the range $0 \leq \mathrm{L/D} \leq 25$. As a strictly unimodal function with a known extremum within the interval, this approach will converge to the global optimum.

For the case, $\tau = 0.125$, we find that the maximum lift to drag ratio is $\mathrm{L/D_{max}} \approx 5.4$, as shown in Table 2 and Figure 5. In this case, $a = -2.30\text{e}{-2}$, $b = -3.77\text{e}{-6}$, $e = -3.96\text{e}{-2}$, and $f = -2.14\text{e}{-6}$. The relaxation variable, $r = 7.53\text{e}{-3}$ with an error of $\epsilon = 1\text{e}{-5}$.

	Convex Approximation	Numerical Integration	Error
c_l	9.853e−3	9.945e−2	0.93%
c_d	1.828e−3	1.829e−3	0.05%
L/D	5.39	5.44	0.92%

Table 2 Convex approximation vs numerical integration values of force coefficients for maximum L/D**.**

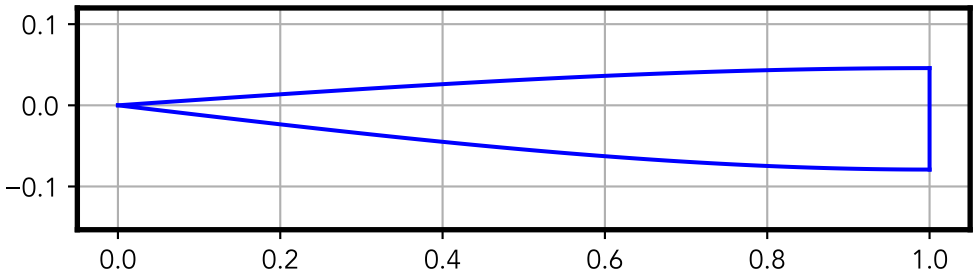

Fig. 5 Maximum L/D **shape for** $\tau = 0.125$**.**

Finally, this approach is particularly useful for generating a Pareto front of the tradeoff between thickness or are and maximum achievable L/D. As shown in Figure 6, for $0.05 \leq \tau \leq 0.25$ it is possible to achieve values of $2 \leq \mathrm{L/D}_{\max} \leq 14$.

VIII. Conclusion

In conclusion, we have presented an extension to the CASO method for inclusion of nonconvex objective functions via variable transformation and relaxation of nonconvex constraints. We have also demonstrated how to implement this technique to obtain globally maximal lift to drag ratio cross sections of hypersonic vehicles defined by multiple cubic polynomials. We have presented a rather simplistic geomtric shape definition in order to ease description of these techniques. However, the approach easily admits more complicated shapes, including those defined as various types of splines (employing linear descriptors) and also discretized surfaces. Additionally, there are a wide variety of geometric constraints, including the ability to contain internally specified volumes, that are applicable, and we have previously described elsewhere. Finally, we have shown that, in representative cases, there is excellent accuracy in the representation of lift and drag coefficient by formulations that are readily used in solvers requiring formatting as disciplined convex optimization problems. We believe this work adds to a number of important techniques for conceptual design exploration studies, especially in the field of hypersonic vehicle development.

References

[1] Boyd, S., and Vandenberghe, L., *Convex Optimization*, Cambridge University Press, 2004.

[2] Hoburg, W., and Abbeel, P., "Geometric Programming for Aircraft Design Optimization," *AIAA Journal*, Vol. 52, No. 11, 2014, pp. 2414–2426. https://doi.org/10.2514/1.J052732.

[3] Martins, J. R. R. A., and Ning, A., *Engineering Design Optimization*, Cambridge University Press, Cambridge, UK, 2021. https://doi.org/10.1017/9781108980647, URL https://mdobook.github.io.

[4] Berkenstock, D., Alonso, J., and Laurent, L., "A Convex Optimization Approach to Thin Airfoil Design," *AIAA AVIATION Forum*, 2022.

[5] Berkenstock, D., Alonso, J., and Laurent, L., "Convex Optimization of Low-Observability Hypersonic Re-Entry Vehicles," *44th IEEE Aerospace Conference*, 2023.

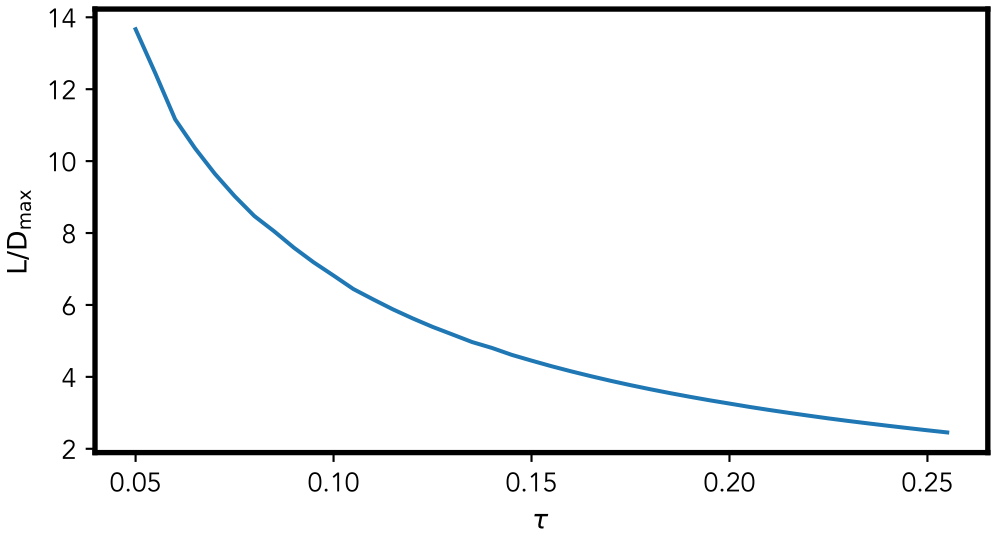

Fig. 6 Maximum L/D as function of τ.

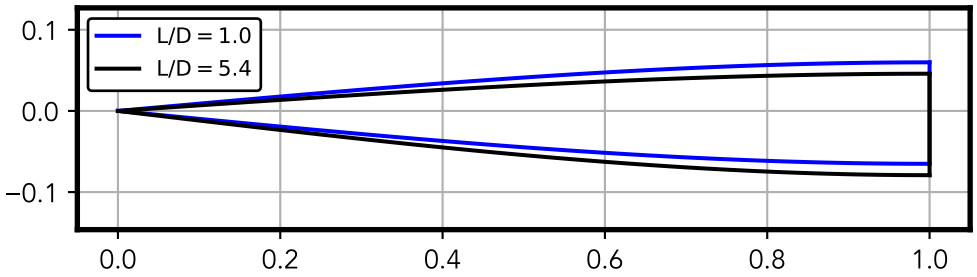

Fig. 7 Maximum L/D shape compared to $L/D = 1$ optimal shape.

[6] Diamond, S., and Boyd, S., "CVXPY: A Python-embedded modeling language for convex optimization," *Journal of Machine Learning Research*, Vol. 17, No. 83, 2016, pp. 1–5.

[7] Agrawal, A., Verschueren, R., Diamond, S., and Boyd, S., "A rewriting system for convex optimization problems," *Journal of Control and Decision*, Vol. 5, No. 1, 2018, pp. 42–60.

[8] Berkenstock, D., and Alonso, J., "Analytic Solutions of Hypersonic Newtonian Flows Over Ellipses," *AIAA SCITECH Forum*, 2022.

[9] Anderson, J., *Fundamentals of Aerodynamics*, Anderson series, McGraw-Hill, 2011.

[10] Liberti, L., and Maculan, N., "Global Optimization: from Theory to Implementation," Springer Science + Business Media, New York, 2006.